ISSN: 2664-9640

Line Mapping Based on Odometer and mpu6050

XiaoYu Liu, Jun Li *

Sichuan University of Science & Engineering, Yibin, 644000, China

Abstract

In recent years, with the rapid development of urban pipelines, the detection technology of inner wall defects of buried pipelines also keeps pace with the times. Many scholars have made great contributions to the detection of inner wall defects of pipelines. The detection of inner wall defects of pipelines not only needs to detect the defects, but also needs to locate the defects. The defect location mainly solves the problem of drawing the movement track of the pipeline inspection and inspection platform in the pipeline. Therefore, this paper uses odometer and mpu6050 attitude sensor to plot the track of the pipeline robot to realize pipeline mapping, and needs to display the attitude of the pipeline inspection platform in real time to prevent rollover.

Keywords

Pipe inner wall defect location ;odometer ;mpu6050; pipeline mapping.

1. Introduction

With the rapid development of urbanization in China, the field of pipeline production and manufacturing has also experienced rapid development. Plastic pipeline is the most outstanding one. Since 1990s, China has successively formulated and promulgated a series of incentive policies and measures to promote the use of plastic pipeline, and vigorously promoted the wide application of plastic pipeline in housing construction, urban municipal engineering, agricultural irrigation and other fields. It strongly promotes the rapid development of China's plastic pipeline industry, and the expected development goals put forward in the Recommendations for the Development of China's Plastic Piping Industry during the Thirteenth Five-Year Plan (2016-2020). With the urbanization construction, the construction of water supply and drainage pipe network and gas pipe network is mainly made of PE plastic pipe. Although the performance of buried PE pipe is excellent, with the increase of service life, aging of pipe materials and construction damage, once an accident occurs, it will have a serious impact on people, and the safety of pipelines is increasingly paid attention to. If the internal condition of the pipeline is detected before the accident happens, the accident can be prevented in time. The water leakage caused by the hole in the left figure of Fig. 1 is only the water leakage point at first. Over time, the water leakage point gradually expands. It may also be caused by construction. However, the explosion caused by cracking in Fig. 1 right figure not only causes waste of water resources in the city, but also causes water cut-off in serious cases. It will affect people's living and living. If the PE drainage pipe leaks, it will be more terrible, causing sewage blockage. If it is not handled properly or even polluting the domestic water, it is very important to carry out regular repair plan for PE buried pipeline and timely eliminate potential safety hazards such as perforation, cracking and deformation of the pipeline, which not only guarantees people's living water and gas, At the same time, the service life of pipeline is prolonged. At present, many scholars have studied the detection of buried pipeline defects, but there are relatively few localization of buried pipeline defects, at the same time, it is very important for pipeline maintenance to obtain the types and locations of defects on the inner surface of pipeline in real time, and this research is mainly aimed at the tracing of pipeline robots to achieve pipeline defect localization.

Fig. 1 Piping Defects

2. Location Principle Based on Wheel Odometer

In this study, the differential wheel is used to build the pipeline detection platform [1]. The two encoders in this experiment are located on the two front wheels of the pipeline detection platform. When the car is moving, the motor turns to drive the encoder to rotate. It should be noted that the speed reduction ratio of the ga12-n20 motor is 1:450. For the counting of the encoder, the data is collected every 50ms, and the conversion from the encoder counting to the left and right wheel speeds is as follows 1:

$$vec(\mathrm{cm/s}) = \frac{\pi * d * 0.1 * \mathrm{Encoder\_Left(Encoder\_Right)}}{a * t} \tag{1}$$

d is the diameter of the wheel, size 33 mm, Encoder_ Left and Encoder_ Right is the count of right and left wheel encoders, A is the number of pulses generated by one turn of motor. This encoder is 7ppr, but the deceleration ratio is 1:450. Therefore, the number of pulses generated by one turn of motor is 3150, t is the sampling time, and 50ms is the sampling time. Because the speed of pipeline detection platform in this study is slow. Therefore, the average speed calculated by 50ms can be taken as instantaneous speed and taken into the kinematic model of two-wheel difference to obtain the instantaneous motion speed and steering angular speed of the pipeline detection platform.

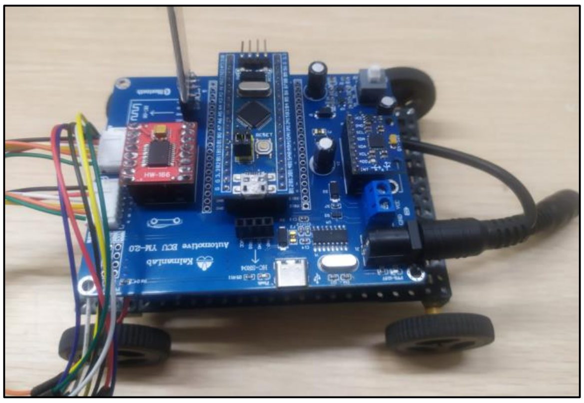

Fig. 2 Pipeline detection platform

In the carrier coordinate system, within the sampling time t, t should be as short as possible, because if there is a turning situation, the shorter t, the more accurate the arc drawn. The sampling time of this upper computer is 50ms, so as to calculate the moving distance in t time, take the position of the original down pipeline detection platform as the position of the world coordinate system, and decompose this distance into the world coordinate system. Formula 2 can be obtained from the kinematic model:

$$\begin{aligned}
&\Delta \mathrm{x} = \Delta d * \cos(\theta) = v * \Delta t * \cos(\theta) \\
&\Delta y = \Delta d * \sin(\theta) = v * \Delta t * \sin(\theta) \\
&\Delta \theta = \mathrm{w} * \Delta t
\end{aligned} \tag{2}$$

By summing the displacement changes in time t on the X and Y axes, the coordinates in the world coordinate system relative to the initial position can be obtained.

$$\begin{aligned}
&\mathrm{x} = x_{\mathrm{on}} + \Delta x = x_{on} + \mathrm{v} * \Delta t * \cos(\theta) \\
&y = y_{on} + \Delta y = y_{on} + \mathrm{v} * \Delta t * \sin(\theta) \\
&\theta = \theta + \mathrm{w} * \Delta t
\end{aligned} \tag{3}$$

Where: x_{on}, y represents the position of the piping robot at the last moment in the world coordinate system, w, V is the line speed at the center of the differential wheel, is the yaw angle, and the heading angle is calculated by mpu6050.

3. Fusion for attitude angle calculation

3.1. Attitude Solution Using Accelerometers

Due to the influence of gravity, the acceleration of gravity will act at rest, but note that the acceleration vector of the accelerometer response is opposite to the current direction of force, so the acceleration of the z-axis at rest should be g. In the initial coordinate system, according to the rotation sequence of ZYX [2], the coordinates of (0, 0, g) in the new coordinate system can be calculated, and the rotation matrix can be multiplied to the left. Gravity is then obtained in the new carrier coordinate system, e.g. Formula 4.

$$\begin{aligned}
\begin{bmatrix} \mathrm{ax} \\ ay \\ az \end{bmatrix} &= \begin{bmatrix} 1 & 0 & 0 \\ 0 & \cos r & \sin r \\ 0 & -\sin r & \cos r \end{bmatrix} \bullet \begin{bmatrix} \cos p & 0 & -\sin p \\ 0 & 1 & 0 \\ \sin p & 0 & \cos p \end{bmatrix} \bullet \begin{bmatrix} \cos y & \sin y & 0 \\ -\sin y & \cos y & 0 \\ 0 & 0 & 1 \end{bmatrix} \bullet \begin{bmatrix} 0 \\ 0 \\ g \end{bmatrix} \\
&= \begin{bmatrix} -\sin p \\ \cos p \bullet \sin r \\ \cos p \bullet \cos r \end{bmatrix} \bullet g
\end{aligned} \tag{4}$$

$$\begin{aligned}
&\mathrm{roll} = \arctan\left(\frac{ay}{az}\right) * 57.2974 \\
&pitch = -\arctan\left(\frac{ax}{\sqrt{ay^2 + az^2}}\right) * 57.2974
\end{aligned} \tag{5}$$

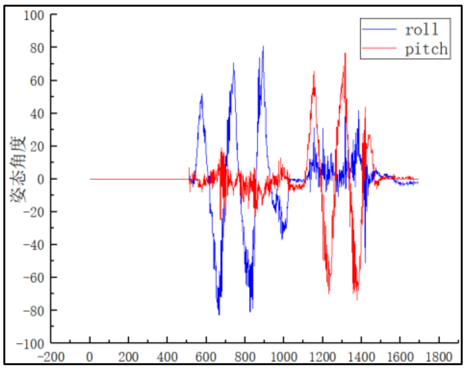

Fig. 3 Calculation of acceleration versus attitude

Solving the above equation, the attitude calculation of accelerometer can be obtained. For example, equation 5 only uses accx, accy and accz to calculate the attitude of motion. The threeaxle attitude calculation formula is as follows: 57.2974 is the alignment of curvature to degree, and 180/pi=57.2974. Since the yaw of course angle can not be referred to by gravity, the course angle can not be calculated only by accelerometer.

3.2. Attitude Solution Using Gyroscope

The gyroscope measures three angular speeds, so it needs to integrate the diagonal speeds. Discrete is the cumulative process. This sample is 50ms. The gyroscope attitude calculation process carries out attitude calculation in the order of ZYX [3]. The current t attitude angle is set as rt, pt, YT and the t+1 attitude angle is set as rt+ Δ R, pt+ Δ P, yt+ Δ Y, the angular velocity also undergoes three rotations, and the calculation of the position and attitude at t+1 moment only needs to add the variation of the position and attitude on the basis of the previous position and attitude. The attitude or the geographic coordinate system is the reference, while the gyroscope reads the angular velocity of the carrier coordinate system, so it needs to be converted, e.g. Formula .

$$\begin{bmatrix} gx \\ gy \\ gz \end{bmatrix} = \begin{bmatrix} 1 & 0 & -\sin p \\ 0 & \cos r & \cos p \bullet \sin r \\ 0 & -\sin r & \cos p \bullet \cos r \end{bmatrix} \bullet \begin{bmatrix} \Delta r \\ \Delta p \\ \Delta y \end{bmatrix} \tag{6}$$

It can be seen from Formula 6 that only the inverse matrix on both sides of the formula can be used to obtain the change of position and attitude, and the inverse matrix on both sides simultaneously. The result is Formula 7:

$$\begin{bmatrix} \Delta r \\ \Delta p \\ \Delta y \end{bmatrix} = \begin{bmatrix} 1 & \sin r \bullet \tan p & \cos r \bullet \tan p \\ 0 & \cos r & -\sin r \\ 0 & \sin r / \cos p & \cos r / \cos p \end{bmatrix} \begin{bmatrix} gx \\ gy \\ gz \end{bmatrix} \tag{7}$$

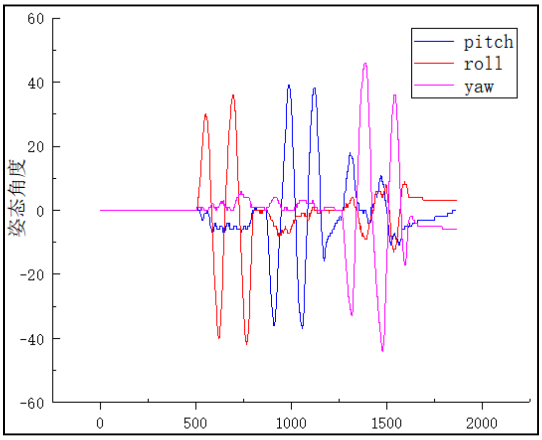

Fig. 4 Gyroscope attitude determination

3.3. Posture Fusion

From the results of acceleration and attitude calculation of gyroscope, we can find that there is a serious burr signal in the acceleration calculation, which indicates that there is high-frequency noise, and after smoothing filtering, the burr can be restrained to a certain extent. The attitude calculation of gyroscope is smooth, but there is drift problem. First remove zero drift, then fuse the attitude of the two. The central idea of complementary filtering is a weight to measure whether attitude believed in acceleration solution is more or gyroscope solution is more. This fusion attempts to compare attitude fusion using complementary filtering and Kalman filter for attitude fusion.

1. Complementary filtering: the gyroscope modifies the last attitude and obtains a new attitude multiplication (1-a)With the attitude multiplied by a (where a is the weight) calculated by the accelerometer, this attempt a=0.2

2. Kalman filter: the system is described by continuously updated state and forecasting correction is carried out continuously during calculation. In this research, attitude measured by accelerometer is used as observation value and attitude calculated by gyroscope is used as forecast value. The gyroscope sensor can integrate and calculate the attitude of the angular rate signal transmitted by itself: while the accelerometer sensor can solve the attitude without offset error under various noises: Kalman filter method can combine the attitude conditions under these two different situations, calculate the Kalman gain, and merge multiple attitudes. The calculation process of Kalman gain is as follows [4].

1. According to the Calman state prediction equation:

$\hat{X}_k^- = A\bullet\hat{X}_{k-1} + B\bullet u_{k-1}$, $\hat{X}_k^-$ for a priori estimate, $\hat{X}_{k-1}$ A posteriori of the previous moment

2.The covariance formula of a prior estimate is as follows:

$P_k^- = A\bullet P_{k-1}\bullet A^T + Q$, P_k^- Covariance Matrix for Prior Estimation, P_{k-1} For the posteriori covariance matrix of the previous moment, Q is the covariance matrix of process noise.

3. The Calman gain formula is as follows:

$K_k = \dfrac{P_k^-\bullet H^T}{H\bullet P_k^-\bullet H^T + R}$, K_k for Kalman gain, R is measuring noise, and is a superparameter

4. The optimal estimation formula is as follows (attitude fusion):

$$X_k = \hat{X}_k^- + K_k\bullet(Z_k - H\bullet\hat{X}_k^-) = \hat{X}_k^- + K_k\bullet(Z_k - \hat{X}_k^-)$$

5. The formula of the posteriori covariance matrix is as follows:

$P_k = (I - K_k H)\bullet P_k^- = (I - K_k)\bullet P_k^-$, P_k for a posteriori covariance matrix

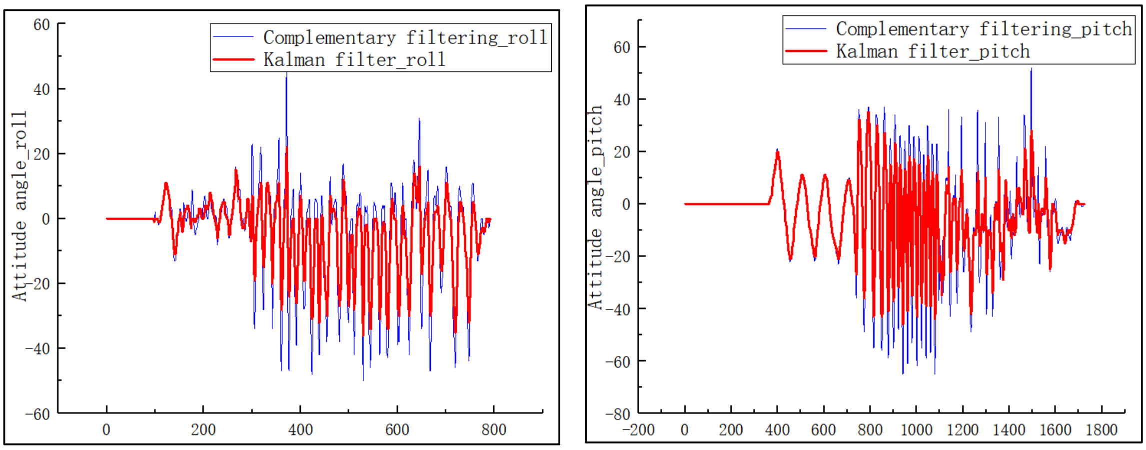

Fig. 5 Comparison between Complementary Filtering and Kalman Filtering References

It can be found that Kalman filter and complementary filter have a high coincidence when the initial roll and pitch swing slightly on the detection platform, and then swing the detection platform rapidly and substantially. It can be found that Kalman filter has a better effect than complementary filter. Therefore, this experiment uses smoothing filter to smooth the original data first. Then Kalman filter is used for attitude fusion.

ISSN: 2664-9640

4. Experimental results

4.1. Attitude solution results

In the previous section, it is analyzed that the difference between Kalman filter and complementary filter is not obvious when the attitude is fused through Kalman filter in small amplitude swing, but it is obvious when it is shaking violently. The effect of Kalman filter is smoother and the filtering effect is more excellent. Therefore, this experiment only shows the effect of Kalman filter. In order to more vividly observe the corresponding relationship between the fused attitude and the physical pipeline detection platform, this time, the anonymous four-axis host computer software is used to display the relationship between the two attitudes in real time, as shown in Figure 5, which represents the three-dimensional display of roll angle, pitch angle pitch and heading angle yaw respectively.

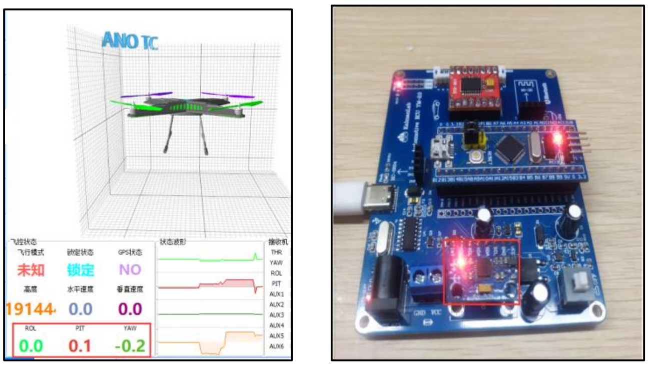

Mpu6050 horizontal placement

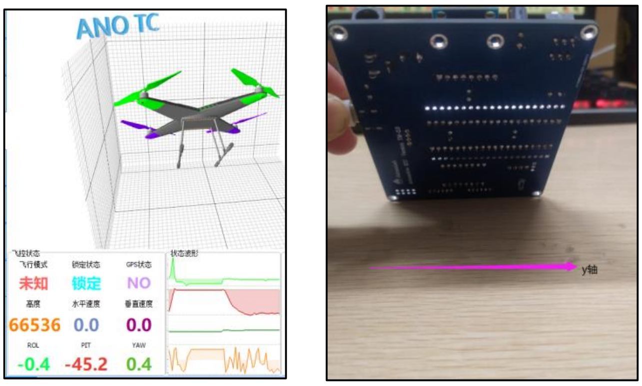

The mpu6050 is tilted 45 degrees around the y-axis pitch

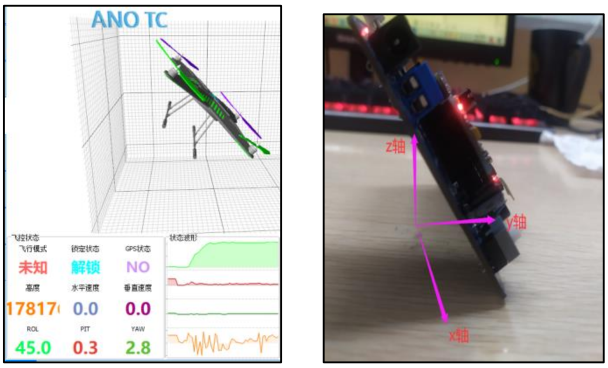

The mpu6050 is tilted 45 degrees around the x-axis roll

Fig.6 attitude 3D display of Kalman filter solution

ISSN: 2664-9640

4.2. Trajectory drawing

In this study, the distance is used to measure the error, and the pipeline detection platform is put into the pipeline to draw the trajectory. The tested pipeline is shown in Figure 6. The pipeline detection is carried out according to the route of the purple arrow in the figure. Because some of the calculated angles are not right angles, the angle is corrected, and the drawn trajectory is shown in Figure 7.

Fig.7 Pipes tested

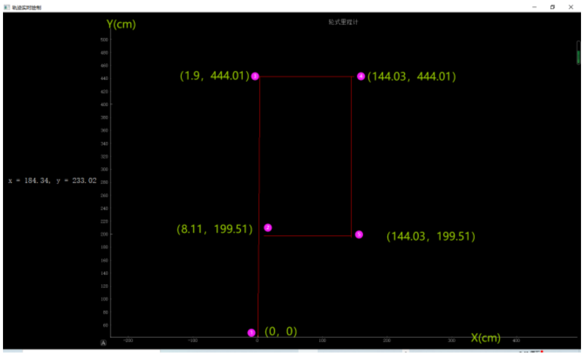

Fig.8 track diagram of detection platform

In the above figure, the actual length of AB pipeline is 210cm, the actual measured length is 199.51cm, the error is 5%, the actual length of BC is 240cm, the actual measured length is 244.5, the error is 2%, the actual length of CD pipeline is 145cm, the actual measured length is 142.13cm, the error is 2%, and the final EF section actually intersects BC, the actual length of EF is 114.5cm, but the trajectory measured length is 135.92cm, the error is 6%.

5. Conclusion

In this study, the odometer and mpu6050 attitude sensor mounted on the pipeline detection platform are used to solve the real-time position and attitude of the pipeline detection platform and draw the motion trajectory of the pipeline detection platform, and good accuracy can be achieved. However, the heading angle in this study has drift, because the heading angle is not fused with Kalman filter attitude, Therefore, the next step of this research is to introduce a 3-axis magnetometer to measure the heading angle, and then conduct attitude fusion with the heading angle calculated by the gyroscope.

References

[1] Zhang Yunwei. Research on gas pipeline inspection robot system and its motion control technology [D]; Shanghai Jiaotong University.

[2] Shen Yue.Research on Pipeline Defect Location Using Accelerometer [J]. Pipeline Technology and Equipment, 2007, (6): 4.

[3] Li Ruitong, Zhao Qingsheng, Wang Xuping. Three-dimensional visualization of pipeline based on inertial sensor data fusion [J]. Science Technology and Engineering, 2018, 18(34): 6.

[4] Deng Hongming, He Yong, Yu Xiaojie, et al. Application of Kalman Filter in UAV Attitude [J]. Automation Technology and Application, 2019, 38(11): 4.